18TH WORLD CONFERENCE ON EARTHQUAKE ENGINEERING
WCEE2024
MILAN

MILAN, ITALY
30TH JUNE - 5TH JULY 2024
www.wcee2024.it

ON THE NECESSARY NUMBER OF AFTERSHOCKS FOR SEISMIC COLLAPSE RISK ASSESSMENT OF BUILDINGS

Saeed Amiri[1], Sanda Koboevic[2]

[1] Department of Civil, Geological and Mining Engineering, Polytechnique Montreal, Montreal, QC, Canada, saeed.amiri@polymtl.ca

[2] Department of Civil Engineering, Polytechnique Montreal, Montreal, QC, Canada

Abstract: *Multiple aftershocks can occur after a severe mainshock and result in considerable cumulative structural damage. This paper aims to determine the number of aftershocks which should be considered in seismic collapse risk assessment of buildings. For this purpose, a probabilistic framework is proposed based on the fragility and hazard analysis. The damage state-dependent fragility is combined with the aftershock probabilistic seismic hazard analysis (APSHA) to assess the collapse risk. Finally, the annual probability of collapse of the mainshock-damaged building is investigated under specific numbers of aftershocks. The application of the framework is then illustrated on a case study, a 4-story RC frame building. The results indicate that the number of aftershocks required to be considered in seismic collapse risk evaluation can be affected by the mainshock magnitude.*

1 Introduction

A major mainshock can trigger several aftershocks during a given time interval, leading to additional structural damage. International seismic codes currently focus only on mainshocks when assessing and designing structures (Araújo et al. 2016; Amiri and Soroushian 2017). In view of the possible cumulative damage inflicted to the structure by mainshock-aftershock sequences, it is of great significance to develop assessment and design procedures that would account for this phenomenon. Several disastrous seismic sequences have been observed in the past decades. The Darfield earthquake in 2010 with the moment magnitude (M_w) 7.1 in New Zealand was followed by two major aftershocks having M_w 6.2 and 6.0, respectively. These sequential ground motions resulted in 100,000 damaged buildings and 185 deaths in Christchurch (Atzori et al. 2012). The M_w 9 2011 Tohoku earthquake that occurred in Japan triggered hundreds of aftershocks with M_w 5 or greater. The impacts of these sequence-type earthquake and aftermath tsunami were catastrophic: 128,530 houses were destroyed and 15,782 people killed (Kazama and Noda 2012). More recently, on Feb. 6, 2023, a severe earthquake with M_w 7.8 hit the Gaziantep, located in the Southern Turkey. Nine hours later, a M_w 7.5 earthquake occurred in Kahramanmaras around 95 km north to the epicenter of the first earthquake, followed by over 7,184 aftershocks. More than 50,000 deaths and around 6,500 collapsed-buildings have been reported in Turkey and in Syria due to these seismic events (Carrera-Cevallos and Carrera-Cevallos 2023; Papazafeiropoulos and Plevris 2023).

The disastrous consequences induced by the above-stated seismic events clearly show that the effect of sequential earthquakes needs to be taken into account in the seismic design and assessment of structures. Several researchers have focused on the impact of aftershocks on the seismic performance of different

structures (e.g., Tesfamariam and Goda 2017., Shokrabadi and Burton 2018., Amiri et al. 2021a, Amiri et al. 2021b., Amiri et al. 2022., Amiri Koboevic 2022., Ruiz-García and Ramos-Cruz 2023) and infrastructures (e.g., Wang et al. 2017., Gidaris et al. 2020., Garakaninezhad et al. 2023., Akpinar et al. 2023). Aftershocks specifically can play a pivotal role in the seismic resilience and recovery process of damaged structures. In this context, determining the number of aftershocks that should be considered in the seismic evaluation is of great importance. In the majority of previous studies, only one aftershock, usually the strongest one, is taken during a seismic sequence for time history analysis of structures. In a few works, two aftershocks were considered after a mainshock (e.g., Amiri et al. 2021a., Zhang et al. 2020., Zhai et al. 2013., Li et al. 2020) for seismic investigation procedure. In reality, numerous aftershocks occur after a major mainshock, and it is necessary to estimate how many aftershocks should be considered in a post-mainshock time interval. The estimation of the required number of aftershocks in seismic assessment of structures can be performed based on the seismic risk approach.

The aim of this paper is to estimate the necessary number of aftershocks based on the seismic collapse risk assessment of buildings. For this purpose, a probabilistic framework is proposed based on the fragility and hazard analysis. The damage state-dependent fragility is combined with the aftershock probabilistic seismic hazard analysis (APSHA) to assess the collapse risk. Finally, the annual probability of collapse of the mainshock-damaged building is investigated under specific numbers of aftershocks. The application of the framework is then illustrated on a 4-story reinforced concrete (RC) frame building.

2 Methodology

The methodology presented in this research work is developed based on the PEER framework for the performance-based earthquake engineering (PBEE). Seismic hazard, fragility and risk analysis are included in the proposed methodology. For this purpose, the hazard of n^{th} aftershock employing APSHA (aftershock probabilistic seismic hazard analysis) (Yeo and Cornell 2009) is computed. Then back-to-back incremental dynamic analyses are conducted to derive damage state-dependent fragility curves, and finally the collapse seismic risk is the product of hazard and fragility results, taking into account the number of aftershocks. The following steps are performed for the proposed methodology:

(a) Seismic hazard analysis

The probability of occurrence of n^{th} aftershock is determined using Equation 1. Then, the exceedance probability of the earthquake intensity measure (IM) for the n^{th} aftershock is obtained and is incorporated with its occurrence probability to determine the hazard of n^{th} aftershock.

$$P(n) = 1 - \sum_{x=0}^{n-1} \frac{[u(t_{\text{interval}})]^x}{x!} e^{-u(t_{\text{interval}})} \quad (1)$$

$P(n)$ is a function of $u(t_{\text{interval}})$, which represents the average number of aftershocks within a time interval, t_{interval}, as given by Equation 2:

$$u(t_{\text{interval}}) = \int_0^{t_{\text{inerval}}} \vartheta_{A|M_E}\, d\tau \quad (2)$$

In this equation, $\vartheta_{A|M_E}$ is the daily rate of aftershocks at the time τ and can be computed from Equation 3. τ is between 0 and t_{interval}, such that the mainshock occurs at initial time, τ=0.

$$\vartheta_{A|M_E} = \frac{10^{a+b(m_E - m_{A,min})} - 10^a}{(\tau + c)^\rho} \quad (3)$$

where m_E is the mainshock magnitude, $m_{A,min}$ is the minimum magnitude of aftershocks considered, *a* and *b* are constant parameters to characterize the distribution of magnitude and *c* and *ρ* stand for constants to describe the temporal decay in the number of aftershocks.

The exceedance probability of the aftershock IM can be calculated using the Aftershock Probabilistic Seismic Hazard Analysis (APSHA), and this computation is expressed mathematically by Equation 4.

$$P(IM_a > im) = \int_{r_{mib}}^{r_{max}} \int_{m_{A,min}}^{m_m} P(IM_a > im|m,r)\, f_M\left(m, m_{A,min}, m_m\right) f_R(r)\, dm\, dr \quad (4)$$

$P(IM_a > im|m,r)$ is the conditional exceedance probability of aftershock IM (IM_a) given the magnitude and distance of aftershock. IM_a follows the lognormal distribution given the magnitude and distance, thus, this probability can be expressed by Equation 5. In this equation, Φ() denotes the standard normal cumulative distribution function, $\mu_{\ln(IM_a)}$ refers to the median of ln(IM_a), and $\sigma_{\ln(IM\text{as})}$ is the standard deviation of ln(IM_a), resulting from an appropriate ground motion prediction equation.

$$P(IM_a > im|m,r) = 1 - \Phi(\frac{\ln(im) - \mu_{\ln(IM_a)}}{\sigma_{\ln(IM_a)}}|m,r) \quad (5)$$

In this equation, $f_R(r)$ is the probability density function (PDF) of distance, and $f_M\left(m, m_{A,min}, m_m\right)$ denotes the PDF of the aftershock magnitude, which depends on $m_{A,min}, m_m$.

The hazard of n^{th} aftershock is the product of its probability of occurrence and the exceedance probability of IM_a:

$$P(IM_a > im)_n = P(IM_a > im)\, P(n) \quad (6)$$

(b) Seismic collapse risk analysis

The probability of transition between different damage states under sequential earthquakes is obtained by the damage state-dependent fragility analysis, requiring back-to-back IDAs. This can be extended for *n*+1 sequences, including a mainshock and *n* aftershocks. The transition probability from damage state *i* to damage state *j* after the n^{th} aftershock, $P\left(DS_j^n \middle| DS_i^{n-1}\right)_{im,n}$ is incorporated with the hazard of n^{th} aftershock, $P(IM_a > im)_n$, to derive seismic risk, which can be obtained from Equations 7 and 8.

$$\lambda_{ij}^n = \begin{cases} \sum_{IM_a} P\left(DS_j^n \middle| DS_i^{n-1}\right) P(DS_i^{n-1})\, P(IM_a)_n & n > 1 \\ \sum_{IM_a} P\left(DS_j^1 \middle| DS_i\right) P(DS_i)\, P(IM_a)_n & n = 1 \end{cases} \quad (7)$$

$$P(DS_i^{n-1}) = \sum_{k=1}^{i} \lambda_{ki}^{n-1} \quad (8)$$

where λ_{ij}^n is the seismic risk associated with the transition from damage state *i* to damage state *j* after the n^{th} aftershock, $P(IM_a)_n$ stands for the hazard of n^{th} aftershock, namely the probability *that* IM_a reaches *im* after n^{th} aftershock, which is calculated using Equation 6. $P\left(DS_j^n \middle| DS_i^{n-1}\right)$ is the probability of reaching the j^{th} damage state after n^{th} aftershock given that the structure stays at the i^{th} damage state after (n-1)th aftershock. Note that *im* is the intensity of n^{th} aftershock. $P(DS_i^{n-1})$ is the probability of reaching the i^{th} damage state after (n-1)th aftershock, which can be computed from Equation 8. $P\left(DS_j^1 \middle| DS_i\right)$ is the transition probability from i^{th} state to j^{th} state under the first aftershock, that is dependent of post-mainshock damage state, namely $P(DS_i)$ in Equation 7 when n=1. It should be noted that in this paper, the collapse damage state is considered as the last damage state for determining the necessary number of aftershocks.

(c) Determination of necessary number of aftershocks

A target collapse risk ($risk_{target}$) is defined based on previous studies (e.g., Sinković et al. 2016). The collapse risk obtained from Equations 7 and 8 for n^{th} aftershock is compared with the defined target risk to estimate the required number of aftershocks. In other words, if the risk value resulted from Equations 7 and 8 is lower than the $risk_{target}$ value, that number of aftershocks is sufficient for seismic risk assessment of structures.

3 Case study

The application of the above-described methodology is illustrated on a case study, a 4-story residential building located in Vancouver, Canada, with RC moment-resisting frames. The frame geometry and design was adopted from the study conducted by Abo El Ezz (2008). The frame has three bays, each 5 m long and the height of each story is 3 m. The elevation view of the studied frame is illustrated in Figure 1. All columns have square cross section 450x450mm, with the same steel reinforcement (4Ø16 + 4Ø12 = 1822.12 mm2). All beams are 600x300 mm. The fundamental vibration period is 0.615 s. More details about this building can be found in works performed by Abo El Ezz (2008) and Abad et al. (2013).

The nonlinear time history analysis is carried out using OpenSees software (Mazzoni et al. 2006). The Ibarra-Medina-Krawinkler (IMK) deterioration model (Ibarra et al. 2005) was used for nonlinear modelling of the structure.

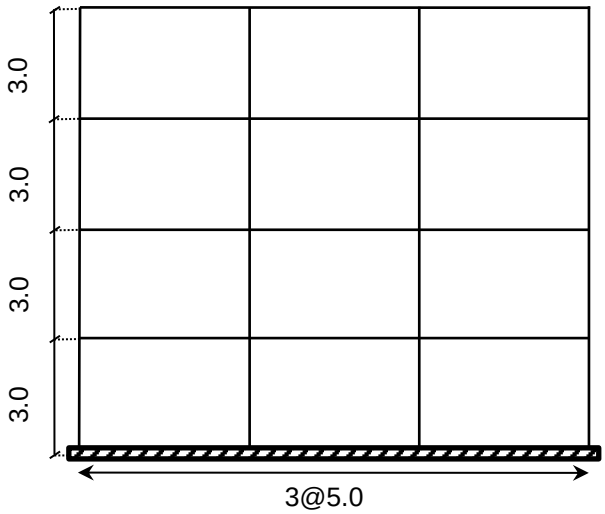

Figure 1. The elevation view of the frame (Abad et al. 2013).

The lumped plasticity approach was applied by employing zero-length elements at the ends of members and the Ibarra-Krawinkler formulation (Ibarra et al. 2005). The back-to-back incremental dynamic analyses under 221 earthquake records were performed to generate damage state-dependent fragility curves. More information about the characteristics of the ground motion records is available in these references (Abo El Ezz 2008 and Abad et al. 2013). Five damage states are considered, from slight state to collapse state (DS_0 to DS_4, respectively). The state transition ($DS_{i\to j}$) can include different combinations, such that i^{th} damage state consists of DS_0 to DS_3, and the range of j^{th} damage state is DS_1 to DS_4. The maximum inter-story drift ratios associated with the given damage states are 0.002, 0.004, 0.01, and 0.018, 0.03 for the slight, moderate, irreparable, severe, and collapse states, respectively (Ghobarah 2004).

4 Seismic risk assessment

An instance of damage-state dependent fragility curves is shown in Figure 2 (a) and Figure 2 (b). In Figure 2 (a), the mainshock-induced damage state is DS_0, while in Figure 2 (b), this initial damage state is DS_2. The initial state of the structure can transit to more severe damage states under aftershocks, namely to DS_1, DS_2, DS_3, DS_4 in Figure 2(a), and to DS_3, DS_4 in Figure 2(b). Moreover, a comparison between collapse fragility curves for two initial damage states of DS_0 and DS_3 is depicted in Figure 2 (c), such that the structure transit to the collapse point from these states. This figure indicates that the exceedance probability of a specific damage state (here the collapse state) tends to increase, as the building experiences more severe damage during the mainshock.

Figure 3 shows the probabilities that n^{th} aftershock can occur during a one-year time interval, as a function of the mainshock magnitude, calculated using Equation 1. It can be seen that the probability of occurrence of aftershocks gradually approaches 1 as the mainshock magnitude increases. For a specific mainshock magnitude, the probability of occurrence of aftershocks decreases, as the number of aftershocks, *n*, increases.

When the mainshock magnitude exceeds 7.5, the occurrence probability of the first to the 15th aftershock is very high, reaching almost 1. In other words, the occurrence of this number of aftershocks is roughly deterministic. This means that as the magnitude of mainshock is greater than a certain value, it is expected that the occurrence probability of aftershocks is independent of the mainshock magnitude.

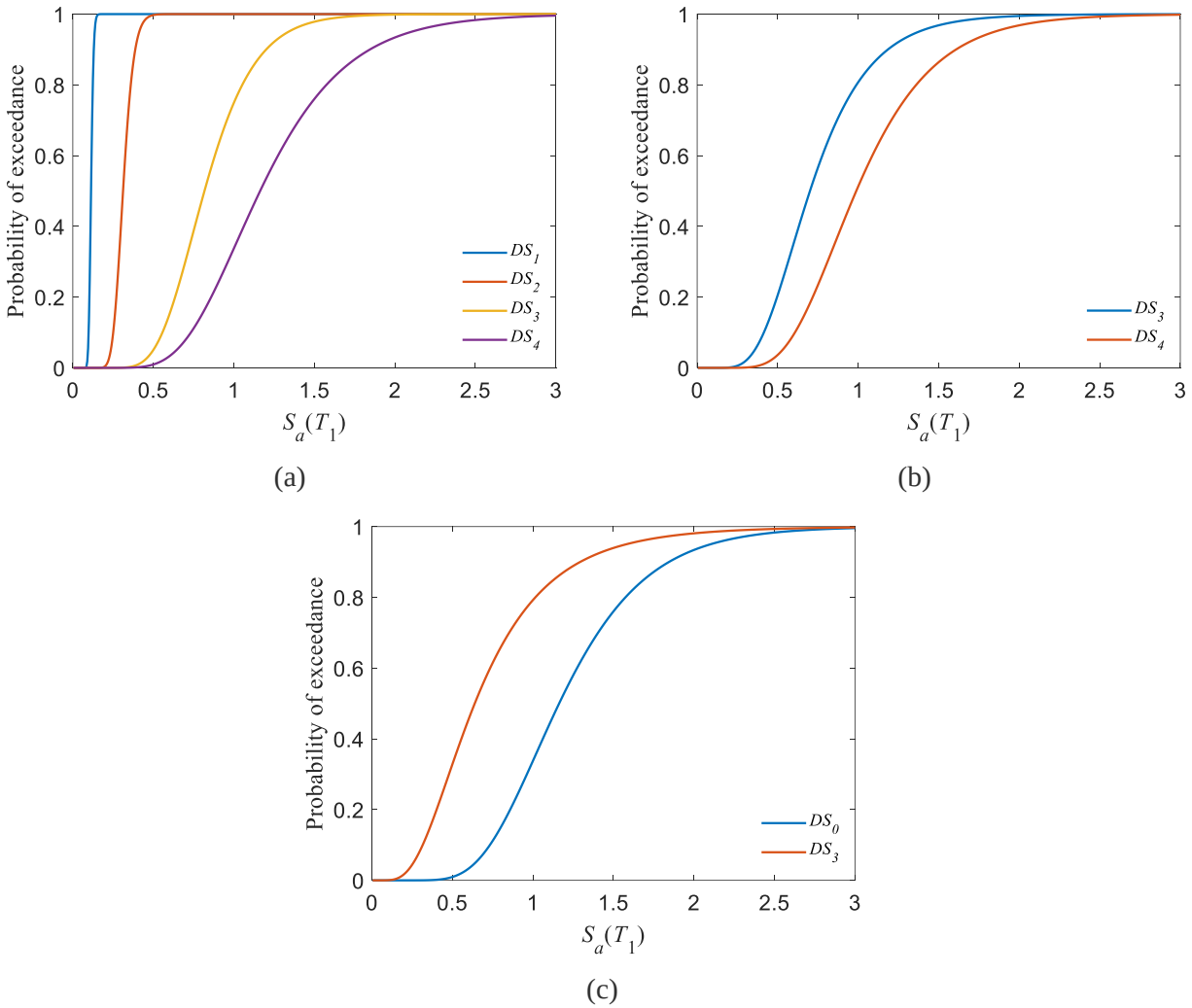

Figure 2. Damage state-dependent fragility curves when the initial damage state is: (a) DS_0, (b) DS_2, (c) comparison between collapse fragility curves for two initial damage states, DS_0 and DS_3.

The APSHA is conducted considering the seismic characteristics of the specified site by varying the number of aftershocks. A 365-day time interval is selected to investigate the aftershock hazard. Figures 4 and 5 show the probability of the structure reaching the collapse state for different numbers of aftershocks (λ_{ij}^n), computed from Equations 7 and 8, considering the mainshock magnitude (M_m) 6.5 and 7.5, respectively. A target risk ($risk_{target}$) of 10^{-4} is considered as a comparison criterion. As shown, this probability (or collapse risk) decreases when the number of aftershocks increases. This stems from the fact that as the number of aftershocks increases, the probability of their occurrence decreases (see Figure 3). It is observed from Figure 4 that the risk value is lower than 10^{-4} (selected as the target risk), if at least 6 aftershocks are considered. Hence, to conduct the risk assessment for the presented case study, it would be necessary to include minimum six aftershocks in the seismic analysis if M_m is equal to 6.5. In the case of M_m=7.5 (Figure 5), this number increases to 11, indicating the at least 11 aftershocks are required to be considered for a risk-based evaluation of the structure.

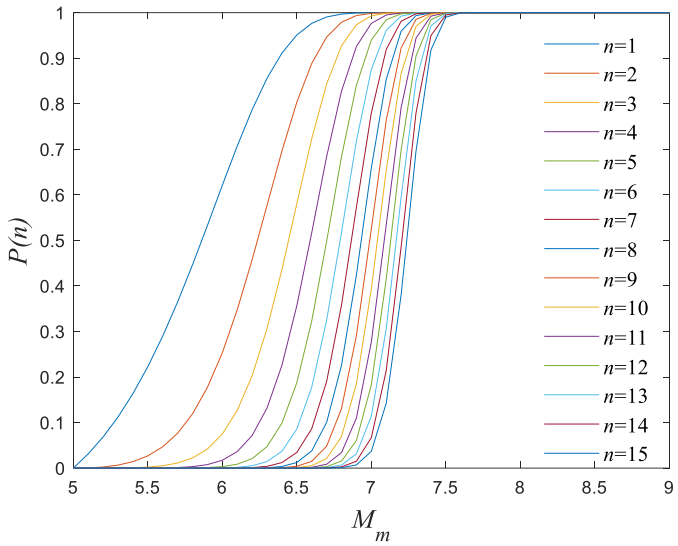

Figure 3. Occurrence probability of multiple aftershocks versus the mainshock magnitude, considering a one-year time interval.

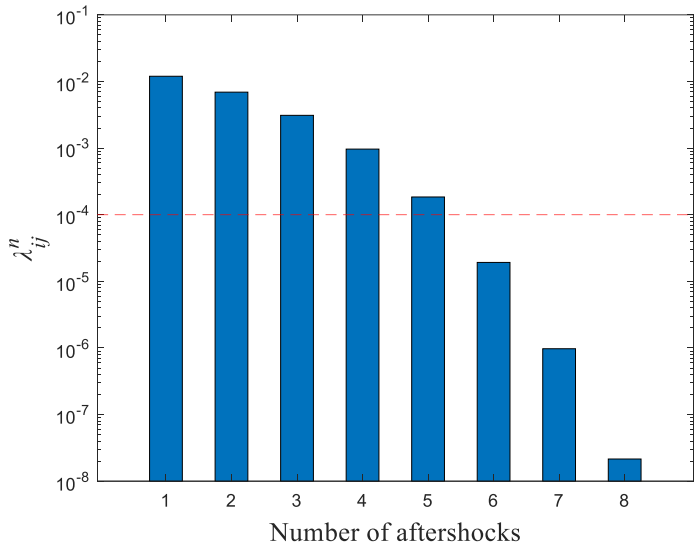

Figure 4. Seismic collapse risk when the moment magnitude of mainshock is 6.5, when the target risk is 10^{-4}.

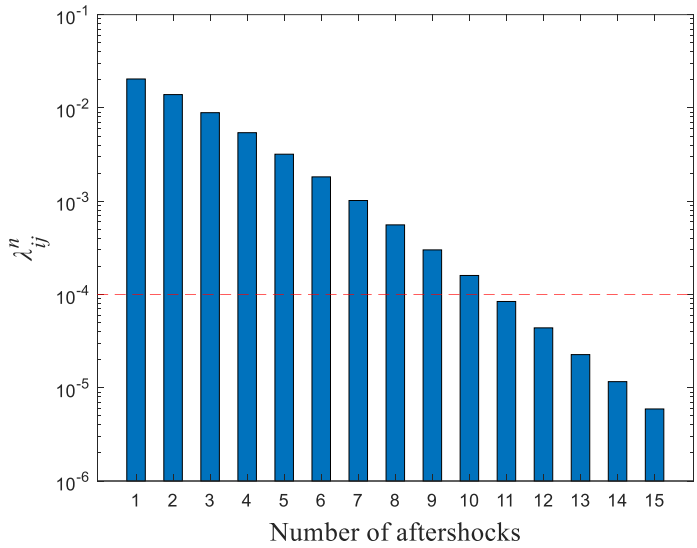

Figure 5. Seismic collapse risk when the moment magnitude of mainshock is 7.5, when the target risk is 10^{-4}.

5 Conclusions

The objective of this paper is to establish the appropriate number of aftershocks to be considered when assessing the seismic collapse risk of buildings. To achieve this aim, a probabilistic framework is introduced, leveraging both fragility and hazard analyses. This approach combines damage state-dependent fragility with the aftershock probabilistic seismic hazard analysis (APSHA) to evaluate the risk of collapse. The proposed framework is then implemented on a case study, a four-story RC frame building. The findings reveal that the occurrence probability of aftershocks declines as the number of aftershocks increases. Additionally, the mainshock magnitude has a significant impact on the determination of the number of aftershocks required to be accounted for in the evaluation of seismic collapse risk, depending on a considered target risk. For instance, with a target risk of 10^{-4} and a mainshock magnitude of 6.5, a minimum of 6 aftershocks should be considered for the annual collapse risk assessment of the case study. However, when M_m is 7.5, this number increases to 11. The study is currently ongoing to further explore the application of the methodology presented for seismic design and risk assessment of structures subjected to sequential earthquakes.

6 Acknowledgements

The financial support of the Natural Sciences and Engineering Research Council of Canada (NSERC) is gratefully acknowledged.

7 References

Abad J., Ulrich T., Réveillère A., Gehl P. (2013). Development of damage state-dependent fragility functions for a MDOF structure through dynamic analyses with successive un-scaled time-histories, *Vienna Congress on Recent Advances in Earthquake Engineering and Structural Dynamics (VEESD)*, Vienna, Austria.

Abo El Ezz A. (2008). *Deformation and strength based assessment of seismic failure mechanisms for existing RC frame buildings*., Doctoral dissertation, ROSE School.

Akpinar U., Arici Y., Binici B. (2023). Post-earthquake effects on the seismic performance of concrete gravity dams, *Structure and Infrastructure Engineering*, 1-4.

Amiri S., Di Sarno L., Garakaninezhad A. (2021a). On the aftershock polarity to assess residual displacement demands, *Soil Dynamics and Earthquake Engineering*, 150: 106932.

Amiri S., Garakaninezhad A., Bojórquez E. (2021b). Normalized residual displacement spectra for post-mainshock assessment of structures subjected to aftershocks, *Earthquake Engineering and Engineering Vibration*, 20: 403-421.

Amiri S., Di Sarno L., Garakaninezhad A. (2022). Correlation between non-spectral and cumulative-based ground motion intensity measures and demands of structures under mainshock-aftershock seismic sequences considering the effects of incident angles, *Structures*, 46: 1209-1223.

Amiri S., Koboevic S. (2022). *Inelastic spectra under mainshock-multiple aftershock sequences*, *Proceedings of the 3rd European Conference on Earthquake Engineering & Seismology*, Bucharest, Romania.

Amiri S., Soroushian A. (2017) A brief review on building structural analysis regulations in different seismic codes, *Res Bull Seismol Earthquake Eng*, 20(1): 1–24 (in Persian).

Araújo M., Macedo L., Marques M., Castro JM. (2016). Code‐based record selection methods for seismic performance assessment of buildings, *Earthquake Engineering & Structural Dynamics*, 45(1): 129-148.

Atzori S., Tolomei C., Antonioli A., Merryman Boncori J.P., Bannister S., Trasatti E., Pasquali P., Salvi S. (2012). The 2010–2011 Canterbury, New Zealand, seismic sequence: Multiple source analysis from InSAR data and modeling, *Journal of Geophysical Research: Solid Earth*, 117(B8).

Carrera-Cevallos A., Carrera-Cevallos D. (2023). The Hit of Two Earthquakes in Turkey-Syria: $\boldsymbol{Mw}$= **7.8** Giziantep-$\boldsymbol{Mw}$= **7.5** Kahramanmaras, *Available at SSRN 4392215*.

Garakaninezhad A., Amiri S., Noroozinejad Farsangi E. (2023). Effects of Ground Motion Incident Angle on Inelastic Seismic Demands of Skewed Bridges Subjected to Mainshock–Aftershock Sequences, *Practice Periodical on Structural Design and Construction*, 28(2): 04023006.

Ghobarah A. (2004). On drift limits associated with different damage levels, *International workshop on performance-based seismic design*, Department of Civil Engineering, McMaster University, Ontario, Canada:

Gidaris I., Padgett J.E., Misra S. (2022). Probabilistic fragility and resilience assessment and sensitivity analysis of bridges incorporating aftershock effects, *Sustainable and Resilient Infrastructure*, 7(1): 17-39.

Ibarra LF., Medina R.A., Krawinkler H. (2005). Hysteretic models that incorporate strength and stiffness deterioration, *Earthquake engineering & structural dynamics*, 34(12): 1489-1511.

Kazama M., Noda T. (2012). Damage statistics (Summary of the 2011 off the Pacific Coast of Tohoku Earthquake damage), *Soils and Foundations*, 52(5): 780-792.

Li X., Wen W., Zhai C. (2020). A probabilistic framework for the economic loss estimation of structures considering multiple aftershocks, *Soil Dynamics and Earthquake Engineering*, 133: 106121.

Mazzoni S., McKenna F., Scott M.H., Fenves G.L. (2006). *OpenSees command language manual*., Pacific earthquake engineering research (PEER) center, 264(1):137-158.

Papazafeiropoulos G., Plevris V. (2023). Kahramanmaras-Gaziantep, Turkiye Mw 7.8 Earthquake on February 6, 2023: Preliminary Report on Strong Ground Motion and Building Response Estimations, *arXiv preprint arXiv*: 2302.13088.

Ruiz-García J., Ramos-Cruz J.M. (2023). Collapse strength ratios for structures under mainshock-aftershock subduction seismic sequences, *Structures*, 56: 104864.

Shokrabadi M, Burton H.V. (2018). Building service life economic loss assessment under sequential seismic events, Earthquake Engineering & Structural Dynamics, 47(9): 1864-81.

Sinković NL., Brozovič M., Dolšek M. (2016). Risk-based seismic design for collapse safety, *Earthquake Engineering & Structural Dynamics*, 45(9): 1451-1471.

Tesfamariam S., Goda K. (2017). Energy-Based Seismic Risk Evaluation of Tall Reinforced Concrete Building in Vancouver, BC, Canada, under M_w9 Megathrust Subduction Earthquakes and Aftershocks. *Frontiers in Built Environment*, 3, 29.

Wang G., Wang Y., Lu W., Yan P., Zhou W., Chen M. (2017). Damage demand assessment of mainshock-damaged concrete gravity dams subjected to aftershocks, *Soil Dynamics and Earthquake Engineering*, 98: 141-154.

Yeo GL., Cornell C.A. (2009). A probabilistic framework for quantification of aftershock ground-motion hazard in California: Methodology and parametric study, *Earthquake Engineering & Structural Dynamics*, 38(1): 45-60.

Zhai CH., Wen W.P., Chen Z., Li S., Xie L.L. (2013). Damage spectra for the mainshock–aftershock sequence-type ground motions, *Soil Dynamics and Earthquake Engineering*, 45: 1-12.

Zhang L., Goda K., De Luca F., De Risi R. (2020). Mainshock-aftershock state-dependent fragility curves: A case of wood-frame houses in British Columbia, Canada, *Earthquake Engineering & Structural Dynamics*, 49(9): 884-903.